Preparation of single wall carbon nanotube-pyrene 3D hybrid nanomaterial and its sensor response to ammonia

ŞENOCAK, Ahmet, GÖL, Cem, BASOVA, Tamara V., DEMIRBAŞ, Erhan, DURMUŞ, Mahmut, AL-SAGUR, Hadi, KADEM, Burak and HASSAN, Aseel <http://orcid.org/0000-0002-7891-8087>

Published version

ŞENOCAK, Ahmet, GÖL, Cem, BASOVA, Tamara V., DEMIRBAŞ, Erhan, DURMUŞ, Mahmut, AL-SAGUR, Hadi, KADEM, Burak and HASSAN, Aseel (2018). Preparation of single wall carbon nanotube-pyrene 3D hybrid nanomaterial and its sensor response to ammonia. Sensors and Actuators B: Chemical, 256, 853-860.

Preparation of Single Wall Carbon Nanotube-Pyrene 3D Hybrid Nanomaterial and Its Sensor Response to Ammonia

Ahmet Şenocak[1], Cem Göl[2], Tamara V. Basova[3,4*],

Erhan Demirbaş[1], Mahmut Durmuş[1,*], Hadi Al-Sagur[5], Burak Kadem[5], Aseel Hassan[5]

[1]*Gebze Technical University, Department of Chemistry, Gebze, Kocaeli 41400, Turkey*

[2]*Abant Izzet Baysal University, Innovative Food Technologies Development Application and Research Center, Gölköy, Bolu 14300, Turkey*

[3]*Nikolaev Institutes of Inorganic Chemistry SB RAS, Lavrentiev Pr. 3, Novosibirsk 630090, Russia*

[4]*Novosibirsk State University, Pirogova Str. 2, Russia*

[5]*Material and Engineering Research Institute, Sheffield Hallam University, UK*

* Author for correspondence:

Dr. Mahmut Durmuş, Department of Chemistry, Gebze Technical University, Gebze 41400, Kocaeli, Turkey

Tel: 00 90 262 6053019

Fax: 00 90 262 6053105

E-mail: durmus@gtu.edu.tr

Abstract

In this work, the structural features and sensor response toward ammonia of a three dimensional (3D) SWCNTs material covalently functionalised with 1,6-diethynylpyrene were studied. The target SWCNTs hybrid material was prepared by the reaction of azido substituted SWCNTs with the 1,6-diethynylpyrene containing double terminal alkyne groups *via* the azide-alkyne Huisgen cycloaddition (Click) reaction. The structure of the 1,6-diethynylpyrene compound was determined by different spectroscopic methods such as FT-IR, ^{1}H-NMR, MALDI-TOF mass, fluorescence and UV–Visible, while its SWCNT-Pyrene 3D hybrid material was characterized by FT-IR, Raman, UV-Visible spectroscopies and thermogravimetric analysis. The morphology of the hybrid films was investigated by scanning electron microscope (SEM). The sensing performance of the SWCNT-Pyrene 3D hybrid material was studied against low-concentrations of NH_3 in the range of 0.1-40 ppm by measuring changes in the films' conductivity at different levels of relative humidity. The reversible electrical sensor response toward ammonia was observed both in the case of SWCNT and SWCNT-Pyrene 3D hybrid films however the response values of SWCNT-Pyrene 3D hybrid film were higher than those of SWCNT.

Keywords: 3D Carbon nanomaterials; Pyrene; Covalent functionalization; Chemiresistive sensors; Ammonia vapour.

1. Introduction

About 80% of commercially produced ammonia (NH_3) is used in fertilizers, with the remainder used in a variety of applications such as plastics, synthetic fibers and resins, pharmaceuticals, explosives, refrigeration, and household cleaners [1]. Ammonia is the most common indoor air pollutant; it is a great pollution source to environment and harmful to human health [2]. Ammonia is known to be potentially associated with chronic diseases such as asthma, severe respiratory tract inflammation and lung diseases [3, 4]. Since ammonia is a low boiling compound and volatile, it is very important to develop sensitive devices to detect gaseous NH_3 molecules.

With the rapid development of nanotechnology, hybrid materials play vital role in these new technologies due to the synergetic combination of two or more components, in order to develop different kinds of functional materials possessing distinctive electrical, optical, or mechanical properties [5]. Moreover, functioning of carbon nanotubes (CNTs) are feasible for use in different type of sensors, especially for gases and chemical vapors due to their high electrical conductivity, large surface area and ease of functionalization with different chemical groups [6]. Various research groups have focused on studying and improving the response of CNT-based sensors, however, pristine CNTs have some disadvantages, which include their poor solubility and dispersibility as well as the low recovery at room temperature [7]. Until today, SWCNTs have shown sensitivity toward gases such as NH_3, NO_2, H_2, CH_4, CO, SO_2, H_2S, H_2O_2 and O_2 [8-11]. Researchers have focused on a wide variety of functional groups to be attached either covalently or non-covalently to the CNTs in order to develop CNT-based sensors that are more specific and selective to certain gases or chemical analytes [12]. Carbon nanotubes can be converted to 3D structures such as in the case cross-linked polymers. It is desirable to stack two-dimensional (2D) SWCNT networks to a three-dimensional (3D) architecture because sensitivity and responsivity can improve by incorporating and exposing more nanotubes to gas molecules [13].

Aromatic compounds such as conjugated polymers, porphyrins and pyrene derivatives, are commonly attached to CNT surfaces *via* π-π interaction. Pyrene and its derivatives have been shown to be adsorbed to the CNT surface through a π-π interaction and the resulting nanocomposites are used as building blocks for bonding proteins, polymers and other molecules. In addition, pyrene and its derivatives are well known for their high sensitivity to the local environment [14]. Pyrene has large aromatic system and has been demonstrated to have very high affinity to the surface of CNTs [15]. The formation of Cu (I) -catalyzed 1,2,3-triazoles by efficient coupling of alkyne to pyrene and azide functional MWCNTs has been found to be efficient and very stable and well defined for the coupling of the MWCNTs and the photoactive molecule. On the other hand, because the triazole ring can participate in the hydrogen bonding, the nanoconjugate coupling of pyrene–MWCNTs shows remarkable solubility and stability in aqueous solvents [14].

In this work, the sensing properties of SWCNTs covalently functionalised with 1,6-diethynylpyrene (Fig. 1) toward ammonia were determined. The obtained 3D network structure is thought to provide improved adsorption skeleton for more ammonia molecules. The SWCNTs hybrid materials were prepared by the reaction of azido substituted SWCNTs with the 1,6-diethynylpyrene containing double terminal alkyne groups *via* azide-alkyne Huisgen cycloaddition (Click) reaction. The structure of the 1,6-diethynylpyrene compound was determined by different spectroscopic methods such as FT-IR, ^{1}H-NMR, MALDI-TOF mass, fluorescence and UV–Visible. Its SWCNT-Pyrene 3D hybrid material was characterized by FT-IR, Raman and UV-Visible spectroscopies and thermogravimetric analysis. The morphology of the hybrid films was investigated using scanning electron microscopy (SEM). The electrical response of SWCNT-3D hybrid material towards low concentration of ammonia (0.1-40 ppm) was demonstrated.

2. Experimental details

2.1. Materials

All the reagents and solvents were of reagent grade quality. Sodium L-ascorbate was purchased from Alfa Aeser. SWCNT, pyrene, bromine, $PdCl_2(PPh_3)_2$, trimethylamine, K_2CO_3 and ICl were purchased from Aldrich. Sodium azide and copper(II) sulfate pentahydrate were supplied from Merck. SWCNT–N3 was prepared as reported in our recently published work [16].

2.2. Synthesis

2.2.1. Preparation of 1,6-diethynylpyrene

1,6-Diethynylpyrene was prepared as suggested in the work of Ohshita et al [17]. FT-IR (ν_{max}/cm^{-1}) 3294 (C≡H), 3052 (Ar CH), 2097 (C≡CH), 1182 (Ar C=CH); UV–Vis (THF) λ_{max} nm: 340, 360, 380 and 393. ^{1}H-NMR ($CDCl_3$) δ= 3.59 (s, 2H, HC≡C), 8.11 (d, *J*=9.18 ppm, 4H, ArH), 8.15 (d, *J*=7.85 ppm, 2H, ArH), 8.59 (d, *J*=9.11 ppm, 2H, ArH); ^{13}C-NMR ($CDCl_3$) δ= 82.51 (C≡C), 83.04 (C≡C), 117.28, 122.39, 125.11, 126.31, 128.30, 129.56, 130.54, 131.65; MS (MALDI-TOF) m/z: Calc. for $C_{20}H_{10}$: 250.29. Found: 250.23 $[M]^+$.

2.2.2. Preparation of SWCNTs-Pyrene 3D Hybrid structure

30 mg (0.079 mmol) of 1,6-diethynylpyrene was dissolved in 2 mL DMF and then sonicated for 15 min at room temperature. Meanwhile, 5 mg SWCNT–N3 was suspended separately in 3 mL DMF and sonicated for 30 min at room temperature. The 1,6-diethynylpyrene solution was then added to the SWCNT–N3 suspension dropwise. 1.0 mol% Copper(II) sulfate pentahydrate and 5.0 mol% sodium L-ascorbate were added to this suspension as catalysts at room temperature and the resulting mixture was kept at 60 ^oC for 24 h. Finally, the reaction mixture was centrifuged twice with water, ethanol and dichloromethane in sequence and dried in vacuum.

FTIR ν/cm^{-1}: 3289 (CH triazole ring), 3070 (Aromatic CH), 1576 (C=C), 1180 Ar (C=C)

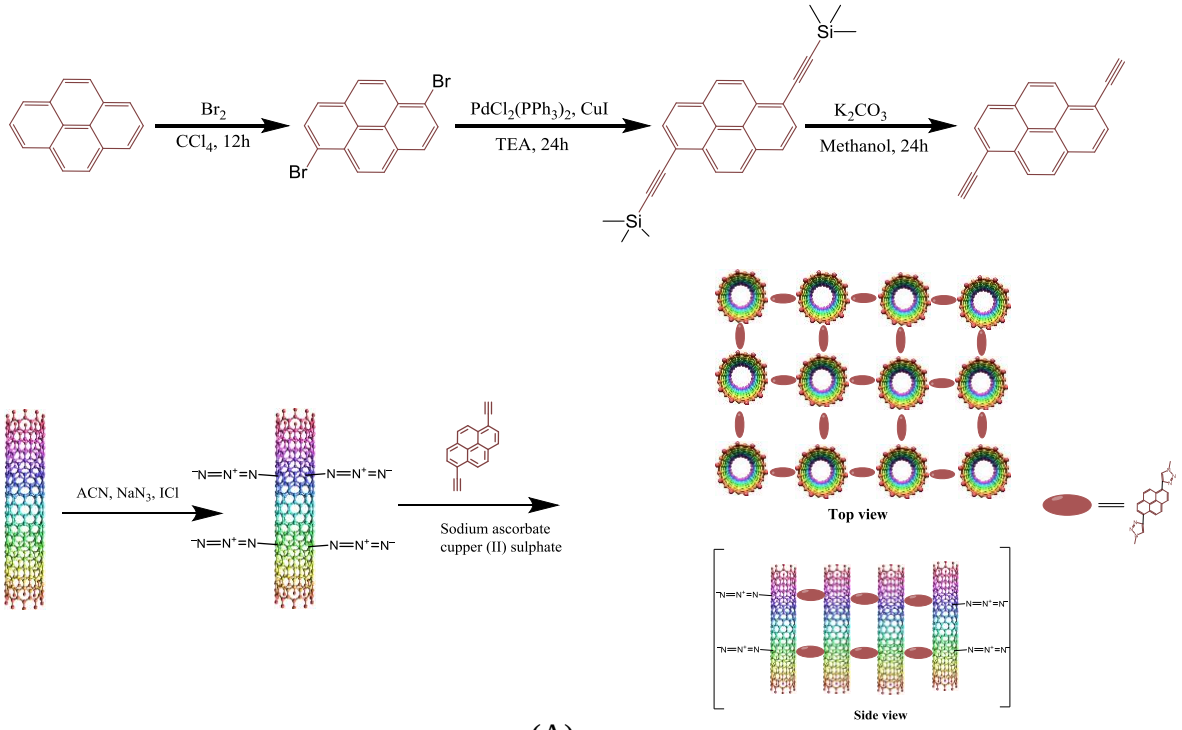

(A)

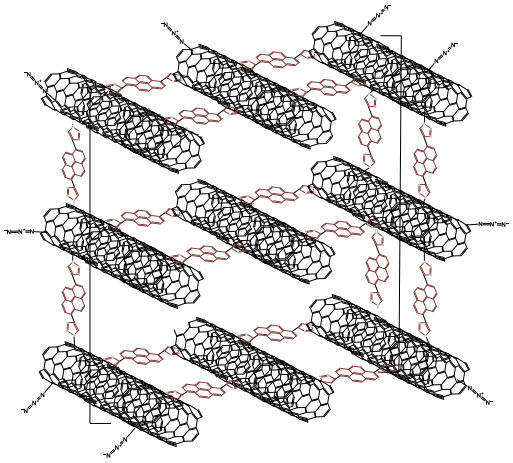

(B)

Figure 1. (A) The synthesis routes of 1,6-diethynylpyrene and covalently 1,6-diethynylpyrene bonded SWCNT-Pyrene 3D hybrid material (B) Proposed 3D structure of the target materials.

2.3. Deposition of thin films and their characterization

Thin films of the hybrid were deposited by drop casting of their suspensions in dichloromethane. The average thickness of the deposited films, estimated by spectroscopic ellipsometry (Woolam M-2000V^{TM} rotating analyser spectroscopic ellipsometer) was about 100 nm.

2.4. Characterization techniques

The structure of the 1,6-diethynylpyrene compound was determined by different spectroscopic methods such as FT-IR, ^{1}H-NMR, MALDI-TOF mass, fluorescence and UV–Visible. The novel SWCNT-Pyrene 3D hybrid material was characterized by FT-IR, Raman and UV-Visible spectroscopies, thermogravimetric analysis and scanning electron microscopy (SEM). FT-IR spectra were recorded on a Perkin Elmer Spectrum 100 spectrophotometer. Raman spectra were recorded with a Triplemate, SPEX spectrometer equipped with CCD detector in back-scattering geometry. 40 mW line of Ar-laser at 488 nm was used for the spectral excitation. ^{1}H-NMR spectrum of 1,6-diethynylpyrene with tetramethylsilane (TMS) as an internal standard was recorded on a Varian 500 MHz spectrometer. The mass spectrum of this compound was recorded by a Matrix Assisted Laser Desorption Ionization (MALDI) BRUKER Microflex LT using 2,5-dihydroxybenzoic acid (DHB) as matrix. UV-visible spectrophotometer (Varian 50-scan UV–visible) in the range of 190-1100 nm was used to measure the absorption spectra. The morphology of the synthesized hybrid material was determined by FEI-Nova scanning electron microscopy (SEM) with high magnification (160,000X) and high voltage (10kV). High-resolution transmission electron microscopy (HRTEM) images were obtained using a JEM-2010 instrument at an accelerating voltage of 200 kV. The 3D hybrid films were prepared by evaporating a drop of hybrid dispersion in dichloromethane on a 200 mesh copper grid covered with a ‘‘holey’’ carbon film. Thermo-gravimetric analyses (TGA) were carried out using a Mettler Toledo STAR^{e} Thermal Analysis System at a rate of 10^{o}C min^{-1} in nitrogen flow of 50 mL min^{-1}. Brunauer–Emmett–Teller (BET) surface area was measured using N_2

adsorption/desorption at 77 K on a Quantachrome Instruments. Samples were pre-treated at 150°C for 3 h under vacuum prior to nitrogen physisorption measurements.

2.5. Sensor Properties

The sensing performance of the films was studied against ammonia in the concentration range 0.1-40 ppm, diluted with air. Pure commercial ammonia gas was used as an analyte source. Air was used as the dilution and carrier-gas source. The films were deposited onto platinum interdigitated electrodes (DropSens, G-IDEPT10) to test their conductivity changes upon interaction with the gaseous ammonia. The electrodes have the following dimensions; gap between digits is 10 μm; number of digits is 125x2 with a digit length of 6760 μm; cell constant is 0.0118 cm^{-1}. The electrical resistance of the films was measured using Keithley 236 electrometer by applying a constant dc voltage of 10 V. Before starting any measurements, the films were held for 10 min under air flow until the resistance reached a steady state value. NH_3 gas (0.1-40 ppm) was then diluted with air and injected into the measurement cell. All gas sensing measurements were carried out at the temperature of 22 ^oC. For humidity measurements, the wet carrier gas was prepared by bubbling the carrier gas through distilled water. The relative humidity (RH) inside the measurement cell was controlled with a commercially available humidity meter (MPE-202.013).

3. Results and Discussion

3.1. Spectral characterization of the materials

The ^1H NMR spectrum of the 1,6-diethynylpyrene showed well-resolved bands as revealed in Fig. 2. The signal belonging to the ethynyl CH proton was observed at 3.59 ppm as a single peak. The aromatic protons were observed at 8.11, 8.15 and 8.59 ppm as doublet peaks.

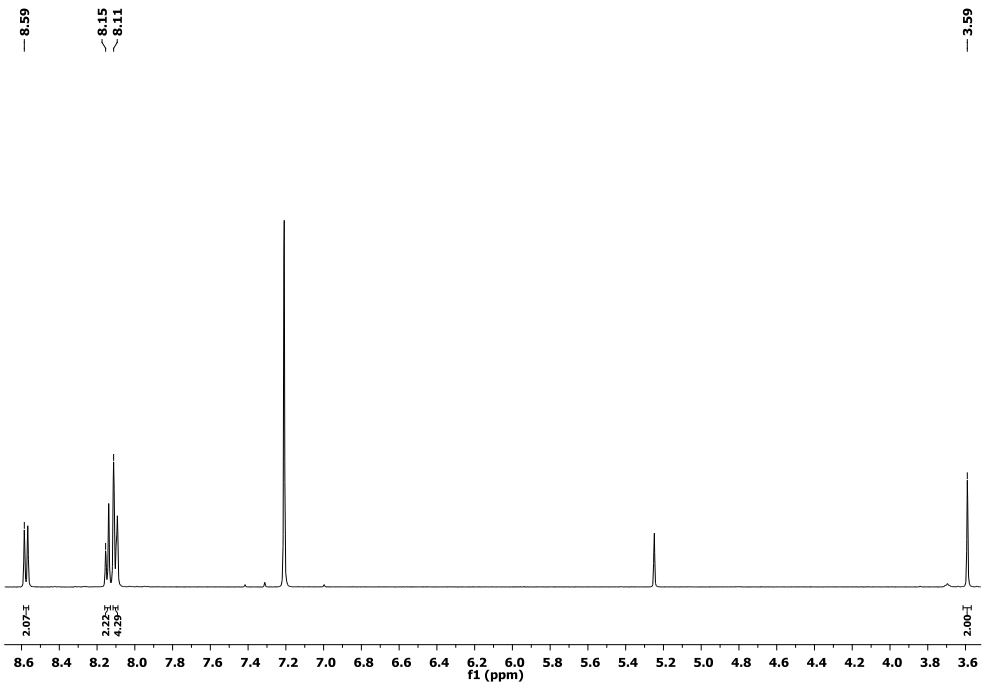

Figure 2. ^{1}H NMR spectrum of 1,6-diethynylpyrene derivative in $CDCl_3$.

The MALDI-TOF mass spectrum of the 1,6-diethynylpyrene showed molecular ion peak at *m/z* = 250.23 as $[M]^+$ supporting the proposed structure of this compound (Fig. 3).

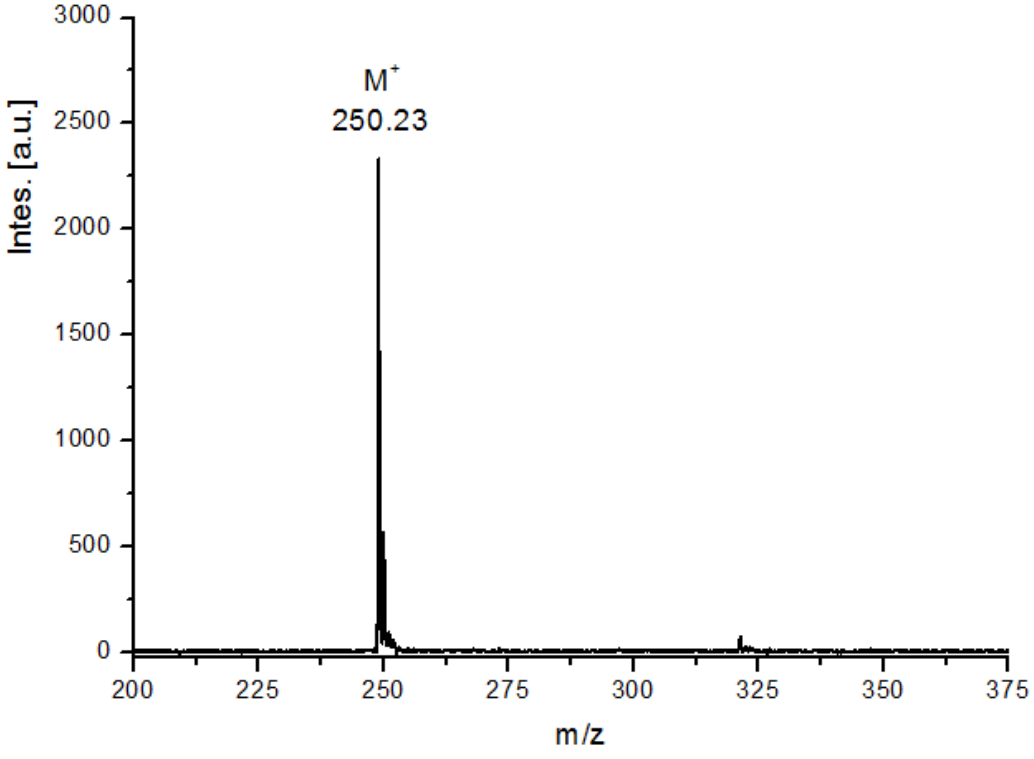

Figure 3. MALDI-TOF spectrum of 1,6-diethynylpyrene compound.

Fig. 4 shows FT-IR spectra of free 1,6-diethynylpyrene, SWCNT-N3 and covalently bonded SWCNTs-Pyrene 3D hybrid. The 1,6-diethynylpyrene compound exhibited vibration peaks at 3294 and 2097 cm^{-1} assigned to H-C≡C- and R-C≡C-R stretching vibrations. On the other hand, the substitution of the -N=N=N groups to SWCNTs was identified with observation of a peak at 2100 cm^{-1} for -N=N=N (azide) vibration in the FT-IR spectrum of SWCNTs-N3. The ≡CH peak for 1,6-diethynylpyrene and -N=N=N peak for SWCNT-N3 in the FT-IR spectra of these compounds disappeared after formation of the covalently bonded SWCNTs-Pyrene 3D hybrid material (Fig. 4). Additionally, the vibration peak for CH stretching of triazole ring was observed at 3289 cm^{-1} which provides a further proof for the functionalization of SWCNTs with 1,6-diethynylpyrene group. On the other hand, a small peak for N=N=N (azide) vibration in the FT-IR spectrum of SWCNTs-Pyrene 3D hybrid material was observed because the azide groups remain at the end of the material.

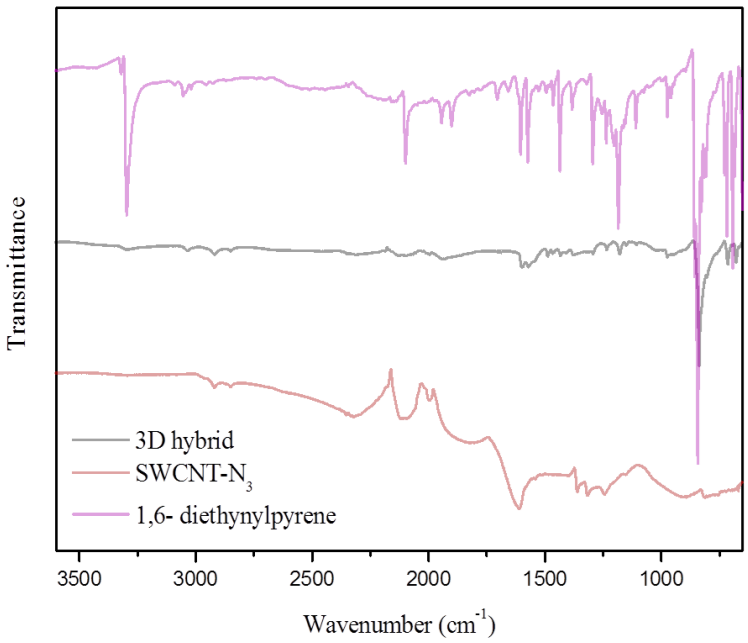

Figure 4. FT-IR spectra of 1,6-diethynylpyrene, SWCNTs-N3 and SWCNT-Pyrene 3D hybrid material.

Raman spectrum of SWCNT-Pyrene 3D hybrid is compared to that of pristine SWCNT as shown in Fig. 5. The ratio of intensities of the radial breathing modes (RBM), disorder (D) mode and graphite mode (G) are used to monitor carbon nanotubes functionalization [18]. The spectrum of SWCNT contains the typical disorder mode D at about 1344 cm^{-1}, and the G band at 1590 cm^{-1}. In the case of SWCNT-Pyrene 3D hybrid the D mode shifts to 1339 cm^{-1} while the G mode shifts to 1583 cm^{-1}. Comparison of the SWCNT-Pyrene 3D spectrum with the spectrum of pyrene derivative shows that the characteristic vibrations of pyrene moiety are shifted noticeably due to interaction with SWCNT. The ratio of the D band to the G band (I_D/I_G) has a value of 0.045 in the spectrum of pure SWCNT, while I_D/I_G value is 0.060 in the SWCNT-Pyrene 3D spectrum.

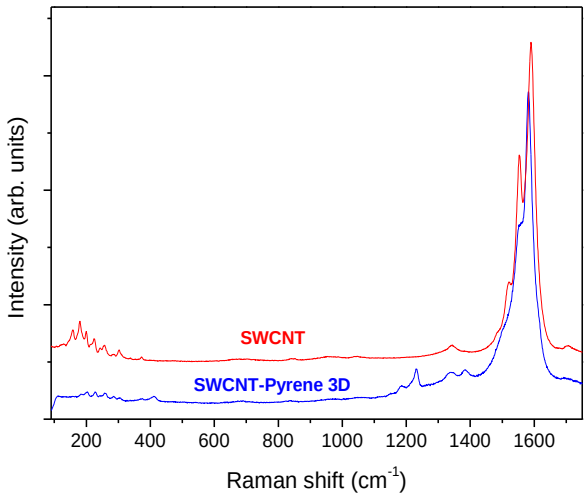

Figure 5. Raman spectra of pristine SWCNT and SWCNT-Pyrene 3D hybrid in the range 90-1700 cm^{-1}.

The RBMs of SWCNT in the range of 158-304 cm^{-1} (Fig. 5) correspond to a distribution of SWCNT diameters in the range from 0.7 to 1.4 nm [19-20]. In the spectrum of SWCNT-Pyrene 3D hybrid the RBMs at 179, 200, 225, 256, 284 and 302 cm^{-1} of SWCNT are shifted to 184, 202, 205, 229, 259, 287, 305 cm^{-1} and their intensities noticeably decrease. All these changes give clear indication to the functionalization of SWCNT with pyrene molecules.

While 1,6-diethynylpyrene compound is soluble in DMF, SWCNTs-Pyrene 3D hybrid material exhibited good dispersion in this solvent. UV–visible absorption spectra of 1,6-diethynylpyrene and its hybrid material are shown in Fig. 6. The spectrum of the 1,6-diethynylpyrene showed characteristic absorption in the bands at 340, 360, 380 and 393 nm in DMF.

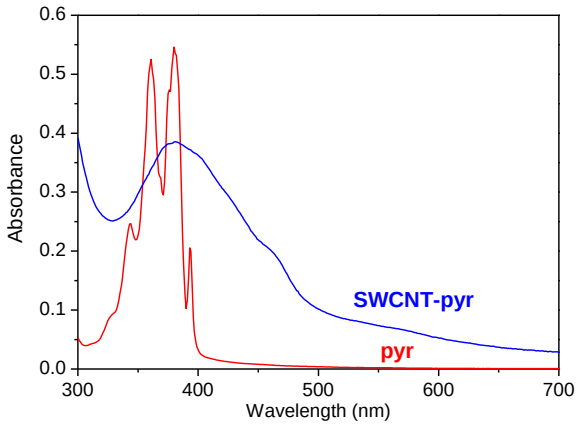

Figure 6. Optical absorption spectra of 1,6-diethynylpyrene compound and SWCNT-Pyrene 3D hybrid in DMF.

In the absorption spectra of SWCNT-Pyrene 3D hybrid, the broad peak with the maximum at 382 nm and the shoulder around 465 nm is shifted to higher wavelength compared to the bands of 1,6-diethynylpyrene. This change might be ascribed to the interaction between SWCNTs and pyrene derivative.

3.2. Thermogravimetric analysis of the hybrid material

Thermogravimetric analysis (TGA) was used to estimate the amount of 1,6-diethynylpyrene molecules covalently anchored on the surface of the carbon nanomaterials (Fig. 7). The TGA data shows a loss of weight about 4.32% for pristine SWCNTs, 10.52% for SWCNT-N_3, 22.02% for SWCNTs-Pyrene 3D and 99.48% for 1,6-diethynylpyrene at 700 °C. The loss of weight observed for pristine SWCNTs between 200 °C and 700 °C may be due to the destruction of the

residual amorphous carbon still present in the nanotubes as well as the decarboxylation of the oxidized species. Weight loss due to the functional groups on SWCNTs is estimated to be 6.20 and 11.50 % for SWCNT-N_3 and SWCNTs-Pyrene 3D, respectively. The number of the azide groups or 1,6-diethynylpyrene molecules on the carbon nanomaterials was calculated as described in the literature [21]. The number of azide functional groups in SWCNT-N_3 was estimated as 1 per 53 carbon atoms. A real ratio of the amount of 1,6-diethynylpyrene molecules covalently anchored on the surface of the nanotubes was 11.56% (11.50%/99.48%). It is estimated that the per 160 carbon atoms on SWCNT-Pyrene 3D hybrids contained one 1,6-diethynylpyrene molecule according to the calculation of ((88.44%x250.29)/(11.56%x12)).

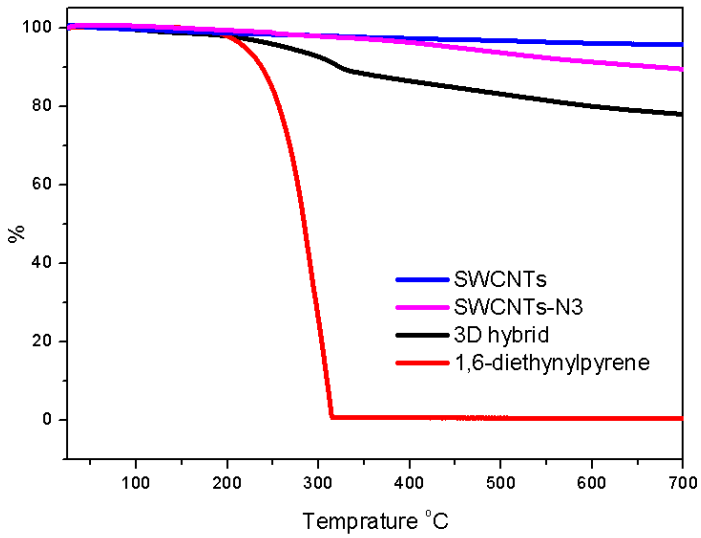

Figure 7. Thermogravimetric analysis of SWCNT-Pyrene 3D hybrid material in comparison with pristine SWCNT, SWCNT-N3 and 1,6-diethynylpyrene.

3.3. Microscopic characterisation of the hybrid material

The morphology of the hybrid films was investigated by scanning electron microscopy (SEM). SEM images of SWCNT and SWCNT-Pyrene 3D films deposited by drop casting of their suspension in DMF are presented in Figs. 8a and 8b. SWCNT-Pyrene 3D hybrids demonstrate different surface morphology compared to bare SWCNT. The SWCNTs clearly exhibit nanotube features on the surface (Fig. 8a), while SWCNT-Pyrene 3D hybrids demonstrate a tendency to

form larger aggregates (Fig. 8b), which can be connected with covalent pyrene bridges between adjacent carbon nanotubes. HRTEM image of SWCNT-Pyrene 3D (Fig. 8(c)) shows a porous assembly of cross-linked carbon nanotubes with pores 1–2 nm in diameter.

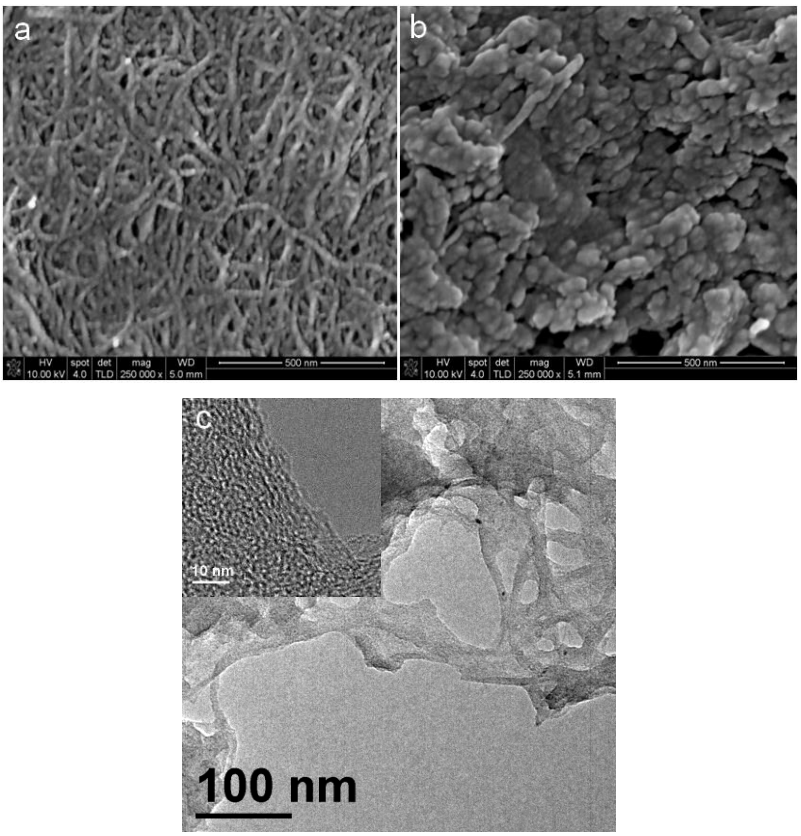

Figure 8. SEM images of the films of SWCNT (a), SWCNT-Pyrene 3D hybrid (b) and HRTEM image of SWCNT-Pyrene 3D hybrid (c).

3.4. Brunauer–Emmett–Teller (BET) analysis

Brunauer–Emmett–Teller (BET) surface area was measured using N_2 adsorption/desorption at 77 K. The BET surface area of both the pristine SWCNTs and SWCNT-Pyrene 3D hybrid material were measured and the results were compared for determination of the effect of 3D pyrene hybrid structure on the surface area. While the surface area of pristine SWCNTs was found 835 m^2g^{-1}, this value increased to 991 m^2g^{-1} for SWCNT-Pyrene 3D hybrid material. According to

BET results, SWCNT-Pyrene 3D hybrid material has more surface area than pristine SWCNTs resulted more NH_3 adsorption.

3.5. Sensor properties

Gas detection study was carried out for thin films of SWCNT and SWCNT-Pyrene 3D films deposited by drop casting onto glass substrates with interdigitated Pt electrodes. The resistance value of the obtained hybrids was around 26 kΩ for SWCNT-Pyrene 3D, which is slightly higher than that measured for pristine SWCNT layers (~20 kΩ).

Fig. 9 demonstrates a typical sensor response $(R-R_o)/R_o$, where R_o is the baseline resistance of the sensor layer of SWCNT or SWCNT-Pyrene 3D hybrid. Injection of NH_3 gas into the chamber leads to a noticeable increase of the films resistance. This type of response is typical for various SWCNT hybrids obtained by covalent and non-covalent functionalization with metal phthalocyanines and other molecules possessing p-type conductivity. Reversible sensor response was observed both in the case of SWCNT and SWCNT-Pyrene 3D hybrid films. The normalized sensor response vs NH_3 concentration is given in Fig. 10. The sensor response of SWCNT-Pyrene 3D hybrid film was more than 9 times higher than that of the pristine SWCNT on exposure to 10 ppm NH_3. It is suggested that the linking groups in SWCNT-Pyrene 3D hybrids prevent formation of close packing of SWCNT in bundles and therefore make the diffusion and penetration of NH_3 molecules inside the 3D structure easier. The exposure area becomes larger in the case of 3D hybrids. On the other hand the aromatic linking groups result in the formation of common aromatic system and therefore facilitate charge transfer between neighbor nanotubes which can also lead to an enhancement of the sensor response.

The response time is almost the same for SWCNT-Pyrene 3D and pristine SWCNT sensors and varies from 5 to 15 s in dependence on the NH_3 concentration. The recovery time for the sensor based on SWCNT-Pyrene 3D hybrid increased from 4 to 20 s when ammonia concentration increased from 0.5 to 10 ppm. The value of the recovery time for SWCNT-Pyrene 3D films is 2

times higher on the average than that for the pristine SWCNT films, however the value is still good for gaseous detection; e.g. for ammonia detection with the concentration of 10 ppm it is equal to 20 s in the case of SWCNT-Pyrene 3D film, while a value of ca. 10 s is observed for the pristine SWCNT film (Fig. 9) for the same gas concentration. The minimal detected concentration of NH_3 in the case of SWCNT films was found to be 10 ppm while that for SWCNT-Pyrene 3D was 0.5 ppm.

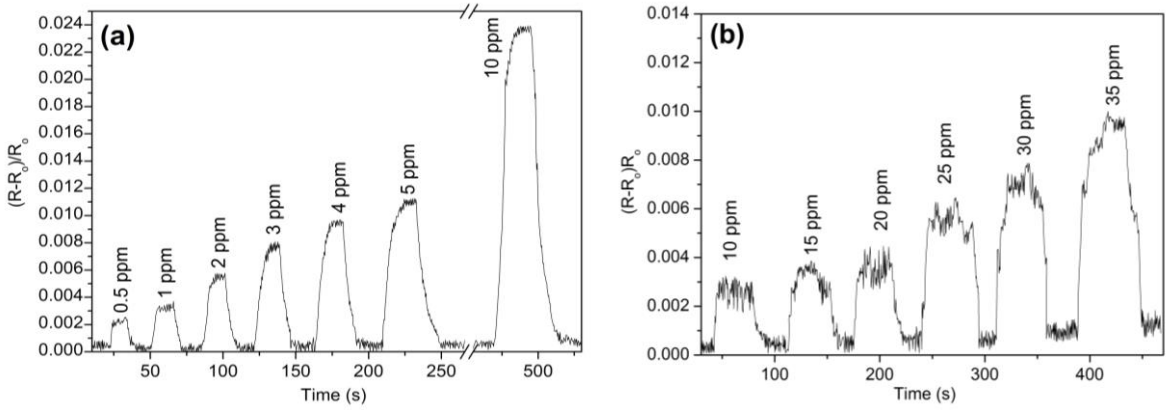

Figure 9. Normalized sensor response of the films of SWCNT-Pyrene 3D (a) and pristine SWCNT (b) vs NH_3.

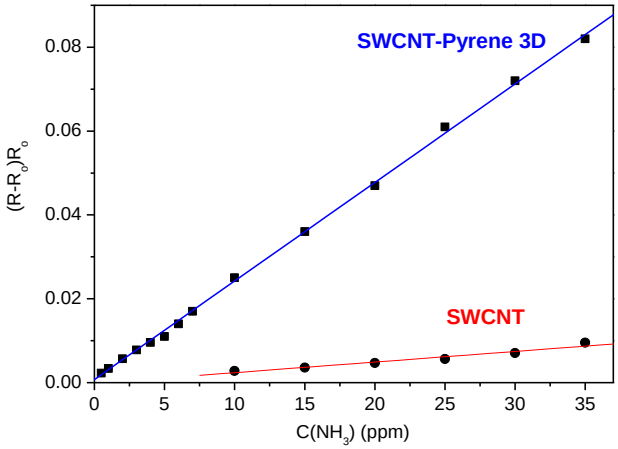

Figure 10. Normalized sensor response vs NH_3 concentration.

To investigate selectivity of the investigated films change in the resistance of both pristine SWCNT and SWCNT-Pyrene 3D films was measured in the presence of ammonia (10 ppm), carbon dioxide (100 ppm), ethanol (500 ppm), toluene (500 ppm), dichlorobenzene (5000 ppm), chloroform (2000 ppm) and NO_2 (0.5 ppm) at room temperature. The interaction of the sensing films with these analytes leads to the increase of the resistance of SWCNT and SWCNT-Pyrene 3D films. A comparative plot of the responses given by the sensor layers to ammonia, carbon dioxide, NO_2 and volatile organic compounds is shown in Fig. 11. SWCNT-Pyrene 3D film shows higher sensitivity to carbon dioxide and volatile organic compounds compared to pristine SWCNT. At the same time its sensitivity to ammonia is noticeably higher compared to the other investigated analytes. This fact makes this material promising for the detection of ammonia in the presence of these analytes.

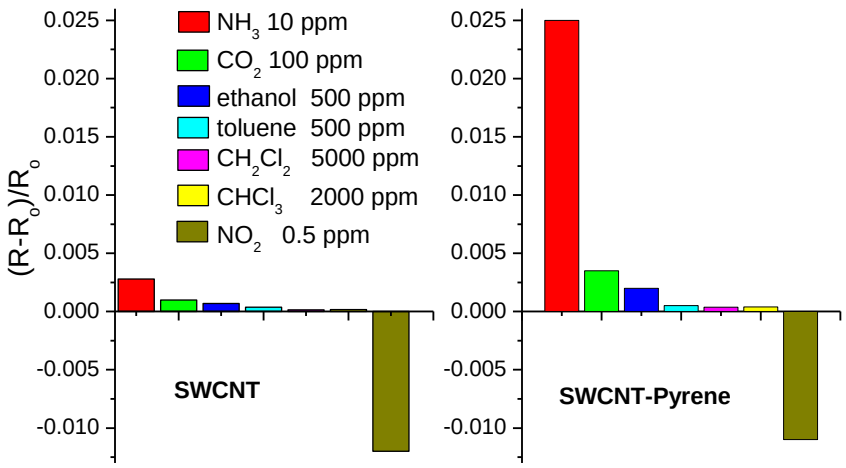

Figure 11. Responses of pristine SWCNT and SWCNT-Pyrene to ammonia (10 ppm), carbon dioxide (100 ppm), ethanol (500 ppm), toluene (500 ppm), dichlorobenzene (5000 ppm), chloroform (2000 ppm) and NO_2 (0.5 ppm).

The interference effect of oxidizing gases has also been studied using NO_2 as an example. In contrast to NH_3, CO_2 and volatile organic compounds the introduction of NO_2 (0.5-5 ppm) to the gas cell leads to a decrease in the resistance of the CNT based gas sensor as demonstrated in Fig.

12 where the sensor is shown to exhibit a strong response towards NO_2. The recovery time is much longer than in the case of ammonia vapors; the resistance does not reach the initial baseline value when the experiments are carried out at room temperature. The problem of recovery of SWCNT-based sensors upon interaction with NO_2 were also highlighted by J. Li et al. [8] and was explained by the higher bonding energy between SWCNTs and NO_2. This issue makes it difficult for the detection of NH_3 in the presence of such oxidizing gas as NO_2, however SWCNT-Pyrene 3D films can be used for the selective detection of ammonia in the presence of reducing gases and volatile organic compounds.

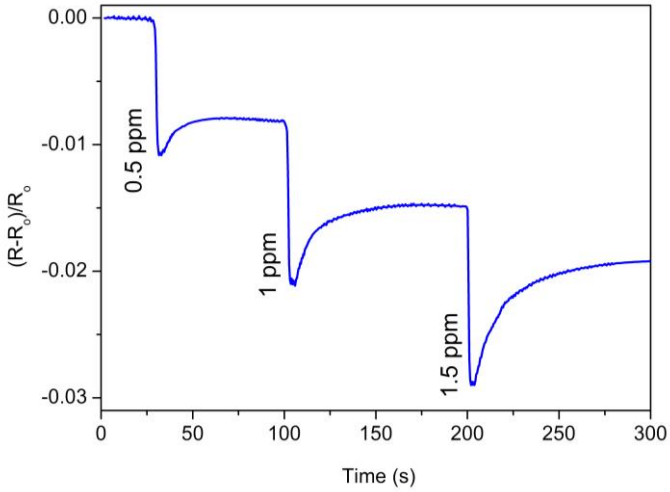

Figure 12. Normalized sensor response of the film of SWCNT-Pyrene 3D toward NO_2.

The other important interfering analyte in the ammonia monitoring is water vapor. Some theoretical modeling and experimental data show that the H_2O molecule has the same reducing effect of NH_3 in the interaction with carbon nanotubes, yielding a charge transfer to CNTs [22]. These charge transfer effects both in the case of H_2O and NH_3 lead to an increase in the resistance of the CNT based gas sensor [23-24], hindering the selective detection of ammonia molecules. To evaluate this interference effect, the sensor performance of SWCNT Pyrene 3D hybrid films was studied at different humidity. The measurements were repeated in the same way in the presence of the relative humidity (RH) of 40 and 70%. The response curves of SWCNT-

Pyrene 3D films to ammonia vapor at the concentration range of 0.5-2 ppm, measured at different RH are given in Fig. 13.

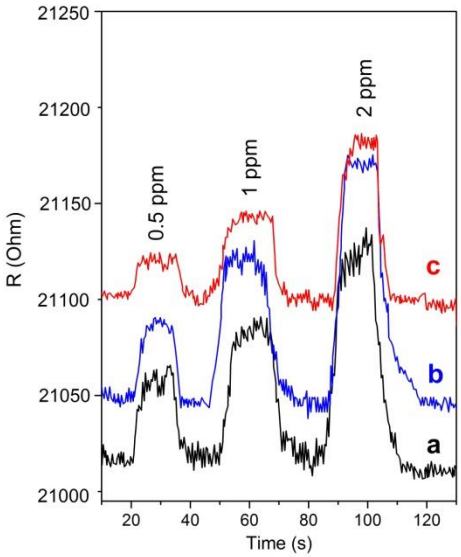

Figure 13. Normalized sensor response of SWCNT- Pyrene 3D films vs NH_3 measured at RH of 0 (a), 40 (b) and 70% (c).

Fig. 13 shows that the initial conductivity of SWCNT-Pyrene 3D film increases with the increase of the RH. The value of the sensor response to dry NH_3 vapour and to NH_3 vapour at the RH 40% is almost the same, whereas it decreases in 1.6-2 times with increasing the RH to 70%. The main reason for the decrease in sensitivity appears to be a competitive sorption of ammonia and water molecules on the surface of the sensing layer.

The sensor reliability is also demonstrated by the reproducibility and stability exhibited by the active film. The reproducibility of SWCNT-Pyrene 3D films was tested by repeating the measurements of their response to ammonia (10 ppm) no less than 30 times. It was shown that the film response was almost constant confirming the reproducibility of the sensor films. The relative standard deviation between the repeated measurements was estimated to be 1.9 %. In order to determine the long-term stability of sensors based on SWCNT-Pyrene 3D films, the sensor response of the same film to ammonia was monitored every 3 days over a period of one month; films subjected to such continuous exposure of 10 ppm ammonia over this prolonged

period have retained 95% of their initial resistance demonstrating highly acceptable sensor stability.

Conclusions

In this work, ammonia gas sensing devices based on SWCNT covalently functionalised with 1,6-diethynylpyrene have been successfully fabricated as three dimensional (3D) network structure for the first time. Electrical sensor response of SWCNT-Pyrene 3D hybrid material toward low concentrations of ammonia (0.1-40 ppm) has been demonstrated. It was shown that the SWCNT-based material covalently functionalised with 1,6-diethynylpyrene exhibits an increase of the sensor response toward NH_3. The detection limit of SWCNT films was found to be 10 ppm while that of SWCNT-Pyrene 3D is 0.5 ppm. The sensing performance of SWCNT-Pyrene 3D hybrid material was also studied by measuring changes in the films' conductivity at different relative humidity values. It was shown that the value of the sensor response to dry NH_3 vapour and to NH_3 vapour at the RH 40% is almost the same; however it decreases by 1.6-2 times with increasing RH to 70%. SWCNT-Pyrene 3D films are shown to be promising active layers for the selective detection of ammonia in the presence of reducing gases and volatile organic compounds.

Compliance with ethical standards

Conflict of interest. The authors declare that they have no conflict of interest.

References

1. P. Wexler, M. Abdollahi, A.D. Peyster, S.C. Gad, H. Greim, S. Harper, V.C. Moser, S. Ray, J. Tarazona, T.J. Wiegand, Encyclopedia of Toxicology, Third Edition (2014) Volume 1.

2. H.Z. Fan, Y.L. Cheng, C.X. Gu, K.W. Zhou, A novel gas sensor of formaldehyde and ammonia based on cross sensitivity of cataluminescence on nano-$Ti_3SnLa_2O_{11}$, Sens. Actuators B. 223 (2016) 921–926.

3. N. Brautbar, M.P. Wu, E. D. Richter, Chronic ammonia inhalation and interstitial pulmonary fibrosis: A case report and review of the literature, Arch. Environ. Health 58 (2003) 592−596.

4. R. E. de la Hoz, D. P. Schlueter, W.N. Rom, Chronic lung disease secondary to ammonia inhalation injury: A report on three cases, Am. J. Ind. Med. 29 (1996) 209−214.

5. Y. Wang, N. Hu, Z. Zhou, D. Xu, Z. Wang, Z. Yang, H. Wei, E.S. Kong, Y. Zhang, Single-walled carbon nanotube/cobalt phthalocyanine derivative hybrid material: preparation, characterization and its gas sensing properties, J. Mater. Chem. 21 (2011) 3779–3787.

6. A.L. Verma, S. Saxena, G.S.S. Saini , V. Gaur, V.K. Jain, Hydrogen peroxide vapor sensor using metal-phthalocyanine functionalized carbon nanotubes, Thin Solid Films 519 (2011) 8144–8148.

7. B. Wang, X. Zhou, Y. Wu, Z. Chen, C. He, Lead phthalocyanine modified carbon nanotubes with enhanced NH_3 sensing performance, Sens. Actuators B 171– 172 (2012) 398– 404.

8. J. Li, Y. Lu, Q. Ye, M. Cinke, J. Han, M. Meyyappan, Carbon nanotube sensors for gas and organic vapor detection, Nano Lett. 3 (2003) 929-933.

9. B. L. Allen, P.D. Kichambare, A. Star, Carbon nanotube field-effect-transistor-based biosensors, Adv. Mater. 19 (2007) 1439-1451.

10. S. N. Kim, J. F. Rusling, F. Papadimitrakopoulos, Carbon nanotubes for electronic and electrochemical detection of biomolecules, Adv. Mater 19 (2007) 3214-3228.

11. D. R. Kauffman, A. Star, Single-Walled Carbon-Nanotube spectroscopic and electronic field-effect transistor measurements: A combined approach, Small 3 (2007) 1324-1429

12. P. Jha, M. Sharma, A. Chouksey, P.Chaturvedi, D. Kumar, G. Upadhyaya, J.S.B.S.Rawat, P.K. Chaudhury, Functionalization of carbon nanotubes with metal phthalocyanine for selective gas sensing application, Synth. React. Inorg. Metal Org. 44 (2014) 1551–1557.

13. H. Li, C. Wen, Y. Zhang, D. Wu, S. Zhang, Z. Qiu, Accelerating gas adsorption on 3D percolating carbon nanotubes, Sci. Rep. 6 (2016) 21313.

14. L. Jing, C. Liang, X. Shi, S. Ye, Y. Xian, Fluorescent probe for Fe(III) based on pyrene grafted multiwalled carbon nanotubes by click reaction, Analyst, 137 (2012) 1718-1722.

15. Y. Gao, M. Shi, R. Zhou, C. Xue, M. Wang, H. Chen, Solvent-dependent fluorescence property of multi-walled carbon nanotubes noncovalently functionalized by pyrene-derivatized polymer, Nanotechnology 20 (2009) 135705 (9pp).

16. B. Kadem, M. Göksel, A. Şenocak, E. Demirbaş, D. Atilla, M. Durmuş, T. Basova, K. Shanmugasundaram, A. Hassan, Effect of covalent and non-covalent linking on the structure, optical and electrical properties of zinc(II) phthalocyanine functionalized carbon nanomaterials, Polyhedron 110 (2016) 37–45.

17. J. Ohshita, K. Yoshimoto, Y. Tada, Y. Harima, A. Kunai, Y. Kunugi, K. Yamashita, Hole-transporting properties of organosilanylene/diethynylpyrene and diethynylanthracene alternating polymers. Applications to patterning of light-emitting images, J. Organomet. Chem. 678 (2003) 33-38.

18. K. A. Wepasnick, B. A. Smith, J. L. Bitter, Chemical and structural characterization of carbon nanotube surfaces, Anal. Bioanal. Chem. 396 (2010) 1003-1014.

19. L. Alvarez, G. De la Fuente, A. Righi, S. Rols, E. Anglaret, J. Sauvajol, E. Munoz, W. Maser, A. Benito and M. Martinez, Diameter dependence of Raman intensities for single-wall carbon nanotubes, Phys. Rev. B. 63 (2001) 153401.

20. D. Huo, L. Yang, C. Hou, H. Fa, X. Luo, Y. Lu, X. Zheng, J. Yang and L. Yang, Molecular interactions of monosulfonate tetraphenylporphyrin (TPPS1) and meso-tetra(4-sulfonatophenyl)porphyrin (TPPS) with dimethyl methylphosphonate (DMMP), Spectrochim. Acta A 74 (2009) 336-341.

21. E.N. Kaya, S. Tuncel, T. Basova, H. Banimuslem, A. Hassan, A.G. Gürek, V. Ahsen, M. Durmuş, Effect of pyrene substitution on the formation and sensor properties of phthalocyanine-single walled carbon nanotube hybrids, Sens. Actuators B 199 (2014) 277–283.

22. J. Zhao, A. Buldum, J. Han, J.P.Lu, Gas molecule adsorption in carbon nanotubes and nanotube bundles, Nanotechnology 13 (2002) 195–200.

23. C.L. Cao, C.G. Hu, L. Fang, S.X. Wang, Y.S. Tian, C.Y. Pan, Humidity sensor based on multi-walled carbon nanotube thin films. J Nanomater 2011 (2011) 707303;

24. E. Steven, W.R. Saleh, V. Lebedev, S.F.A. Acquah, V. Laukhin, R.G. Alamo, J.S. Brooks, Carbon nanotubes on a spider silk scaffold, Nature Comm. 4 (2013) 2435.

Figure Captions

Figure 1. (A) The synthesis routes of 1,6-diethynylpyrene and covalently 1,6-diethynylpyrene bonded SWCNT-Pyrene 3D hybrid material (B) Proposed 3D structure of the target materials.

Figure 2. ^{1}H NMR spectrum of 1,6-diethynylpyrene derivative in $CDCl_3$.

Figure 3. MALDI-TOF spectrum of 1,6-diethynylpyrene compound.

Figure 4. FT-IR spectra of 1,6-diethynylpyrene, SWCNTs-N3 and SWCNT-Pyrene 3D hybrid material.

Figure 5. Raman spectra of pristine SWCNT and SWCNT-Pyrene 3D hybrid in the range 90-1700 cm^{-1}.

Figure 6. Optical absorption spectra of 1,6-diethynylpyrene compound and SWCNT-Pyrene 3D hybrid in DMF.

Figure 7. Thermogravimetric analysis of SWCNT-Pyrene 3D hybrid material in comparison with pristine SWCNT, SWCNT-N3 and 1,6-diethynylpyrene.

Figure 8. SEM images of the films of SWCNT (a), SWCNT-Pyrene 3D hybrid (b) and HRTEM image of SWCNT-Pyrene 3D hybrid (c).

Figure 9. Normalized sensor response of the films of SWCNT-Pyrene 3D (a) and pristine SWCNT (b) vs NH_3.

Figure 10. Normalized sensor response vs NH_3 concentration.

Figure 11. Responses of pristine SWCNT and SWCNT-Pyrene to ammonia (10 ppm), carbon dioxide (100 ppm), ethanol (500 ppm), toluene (500 ppm), dichlorobenzene (5000 ppm), chloroform (2000 ppm) and NO_2 (0.5 ppm).

Figure 12. Normalized sensor response of the film of SWCNT-Pyrene 3D toward NO_2.

Figure 13. Normalized sensor response of SWCNT- Pyrene 3D films vs NH_3 measured at RH of 0 (a), 40 (b) and 70% (c).

Ahmet Şenocak received the BSc and MSc degree from Department of Chemistry of Karadeniz Technical University. He is a PhD student, and Research Assistant at Department of Chemistry Gebze Technical University, Turkey. His research interests are preparation of functional carbon nanomaterials with various molecules and characterization of these materials, for different applications including solar cell, electrochemical properties and sensor etc.

Cem Göl, BSc and MSc in Chemical Engineering, PhD in Chemistry is Assistant Professor at Abant İzzet Baysal University, Innovative Food Technologies Development Application and Research Center (YENİGIDAM), in Turkey. His research interests are the design, synthesis and characterisation of phthalocyanines, borondipyrromethenes (BODIPY), pyrene compounds in a variety of applications such as photodynamic therapy (PDT) of cancer, energy transfer. In addition to this, he is interested in traditional and advanced ceramic materials, as well.

Tamara V. Basova received her Ph.D. (1999) and D.Sc. (2011) in Physical Chemistry from Nikolaev Institute of Inorganic Chemistry, Novosibirsk, Russia. Now, she is a leading researcher in the institute. Her research interests are mainly directed towards the synthesis and characterization of various phthalocyanines and the investigation of the sensor and electrical properties of their oriented films.

Erhan Demirbaş, BSc, MSc, PhD is a Professor at Gebze Technical University, Department of Chemistry in Turkey. His research interests are laser chemistry, adsorption, electrochemistry and chemical sensors, etc.

Mahmut Durmuş, BSc, MSc, PhD is a Professor at Gebze Technical University, Department of Chemistry in Turkey. His research interests are the design, synthesis and characterisation of advanced materials such as phthalocyanines, borondipyrromethenes (BODIPY), coumarins and phosphazenes for different applications including photodynamic therapy (PDT) of cancer, liquid crystals, energy transfer dyes, chemosensors, etc.

Hadi Al-Sagur, BSc, MSc is a lecturer at physiology & medical physics department, Thi Qar university, college of Medicine in the South of Iraq. His research interests are the development of electrochemical glucose biosensors through using different sensing platforms such as graphene-based hydrogels and silica-polyaniline bead-on-bead nanostructures. In addition, study organic dyes for a passive Q-switch laser.

Burak Kadem, BSc, MSc is a PhD student at Sheffield Hallam University, Material and engineering research institute (MERI) in UK. His research interests are organic electronics, solar cells, sensors and composite materials.

Aseel K. Hassan, B.Sc., M.Sc., Ph.D. in Physics, is a Senior Lecturer at the Faculty of Arts, Computing Engineering and Sciences of Sheffield Hallam University, UK. He carries out his research within the Materials and Engineering Research Institute and his interest lies in thin film technology mainly for application in chemical and biosensing, as well as for electronic device application. He uses optical techniques such as surface plasmon resonance and spectroscopic ellipsometry, as well as quartz crystal microbalance detection techniques, employing organic thin films such as metallophthalocyanines and calixarenes as the sensing layers.